Temperature dependence of the indirect absorption edge in AgCl: Evidence of a new source of nonparabolicity in the indirect exciton dispersion*

R. H. Stulen and G. Ascarelli
Physics Department, Purdue University, West Lafayette, Indiana 47907
(Received 28 October 1975)

The temperature dependence of the indirect absorption edge in AgCl has been studied using wavelength modulation over a temperature range from 7 to 80°K. The results show evidence of exciton formation associated with both the valence-band maximum at L and a subsidiary valence-band maximum at Δ. In addition, part of the wavelength-modulation spectrum has been interpreted as being due to nonparabolic effects in the dispersion of the L exciton band. We propose that this nonparabolicity in the exciton dispersion is due to a phonon-induced interaction between the Δ and L exciton bands. We have calculated the expected density of states for the L exciton band assuming that a single phonon is exchanged between the L and Δ exciton bands. The calculated results are in good agreement with experiment.

I. INTRODUCTION

We present in this paper the results of a study of the temperature dependence of the indirect absorption edge in AgCl. The measurements have been made using a wavelength-modulation (WM) technique and span a temperature range from 7 to 80°K. Both the temperature dependence of specific features of the spectrum as well as the line shape of the observed structure have been utilized in the interpretation of the data. The temperature evolution of the spectrum is used to correlate various peaks representing transitions to the same final electronic state in which different momentum conserving phonons are either emitted or absorbed. The line-shape analysis is used both as an aid in identifying the nature of the absorption process, and as a means of accurately determining the threshold energies from exciton formation.

In AgCl different valence-band maxima are predicted[1,2] at points equivalent to

$$\vec{k} = (2\pi/a)(0.5, 0.5, 0.5); \quad \vec{k} = (2\pi/a)(0.5, 0, 0,);$$

$$\vec{k} = (2\pi/a)(0.67, 0.67, 0), \quad \text{and} \quad \vec{k} = (2\pi/a)(0.5, 1, 0).$$

Their energies depend on the choice of parameters used in the calculations. Previous optical[3] and magneto-optical[4] measurements have established that the highest valence-band maximum is at L. The results of our investigation reveal that indirect transitions originate not only from L, but also from the nearly degenerate subsidiary valence-band maximum at Δ. A comparison of the energies of the momentum conserving phonons that take part in the optical absorption process at Δ with the phonon energies given by the dispersion curves derived from neutron scattering data,[5] allows a determination of the magnitude of the wave vector k at which the subsidiary maximum occurs in the $\langle 100 \rangle$ direction.

In addition to the sharply peaked structure associated with the threshold for exciton formation at L and Δ, a large and extremely broad line shape is observed. The vast disparity between the width of the sharp structure and this broad line shape is one of the most striking and intriguing features of the WM spectrum. We have interpreted this broad structure as being due to the nonparabolicity of the exciton band at L which arises through an interaction with the nearly degenerate exciton band at Δ. This interaction gives rise to an enhanced density of states associated with the exciton band at L for energies nearly equal to the exciton gap at Δ.

In Sec. II we discuss briefly the relevant aspects of the experimental details and then proceed in Sec. III to present our results. In Sec. IV we discuss the line shape for the case of a simple parabolic exciton band, and then calculate the exciton dispersion and optical line shape when the interaction of two exciton bands is taken into account.

II. EXPERIMENTAL

Samples were cut from either an ingot of zone-refined AgCl, or an ingot grown by the Bridgman technique. Most of the samples were kindly provided by F. Moser of Eastman Kodak Co. The samples were etched in reagent grade HCl, washed repeatedly in triply distilled water, annealed on a quartz plate at 400°C for 24 h in a He atmosphere, and cooled slowly to room temperature over a period of 48 h. The annealed sample was then polished with a KCN solution, mounted in a cryostat, and cooled slowly to 77°K. Cooling was achieved through exchange gas coupling to a surrounding shield maintained at either liquid-nitrogen or liquid-helium temperature. Through careful control of the exchange gas pressure, both very slow cooling rates and good thermal stability could

be achieved. The initial cool down from room temperature to liquid-nitrogen temperature (LNT), was accomplished at a rate equal to or less than 0.4°K/min. The samples were exposed only to red light while their temperatures exceeded ~100°K.

Wavelength modulation was achieved using a wobbling fused-quartz blade placed immediately after the entrance slit of a model 1700 Spex $\frac{3}{4}$ m monochromator.[6] The light source employed for these measurements was a high-pressure xenon arc. In order to decrease distortions of the spectrum, the modulation depth $\Delta\lambda$ was maintained at a value equal to or less than the spectral slit width of the monochromator.[7] The light emerging from the exit slit was then focused onto the sample, and the transmitted intensity detected by an EMI 9635 photomultiplier. Appropriate filters were used to eliminate stray light. The ac output signal from the photomultiplier passed through a tuned amplifier and was finally synchronously detected. The output of the lock-in amplifier was digitally recorded and simultaneously displayed on a strip chart recorder.

Samples of approximately 0.5-mm thickness were used for the measurements which extended approximately 100 meV into the absorption edge, whereas thicker samples up to approximately 5.0 mm thick were used in studying the structure due to phonon absorption that is seen at higher temperatures. No apparent differences that could not be accounted for by sample thickness were detected in the WM spectrum associated with different samples.

III. RESULTS

The measured wavelength-modulation spectra for temperatures ranging from 11.7 to 60°K, are shown in Fig. 1. The curves are displayed on top of one another for visual clarity and, in addition, are artificially displaced horizontally in order that all of the peaks labeled $L(+\mathrm{TA})$ line up. The scale of energy on the abscissa is therefore only appropriate for the 11.7°K data. The spectra are shown in this way in order to illustrate more clearly the relative shift with respect to $L(+\mathrm{TA})$, of the observed structure. As the temperature increases, the energy gap decreases, and the spectra shift toward lower energy. The temperature dependence of the separation between the peak $L(+\mathrm{TA})$ and the remaining structure of Fig. 1 is plotted in the top portion of Fig. 2. The absolute values of the energy of the $L(+\mathrm{TA})$ peak as a function of temperature are plotted separately in the lower portion of this figure.

From the results shown in Figs. 1 and 2, it is apparent that certain groups of structure move rigidly together as the temperature is varied, indicating that they can be correlated to the same final electronic state. Using this fact and the known phonon energies in the various directions of the Brillouin zone[5] (BZ), we are able to make the following assignments. $L(+\mathrm{TA})$ and $L(+\mathrm{LA})$ are transitions to the exciton band associated with the valence-band maximum at L with the emission of a TA and an LA phonon, respectively. At $T \lesssim 25$°K the width of the peak $L(+\mathrm{TA})$ is instrument limited. At higher temperatures, where the phonon occupation number n is appreciably larger, the same transitions also occur with the absorption of the appropriate phonon. These are labeled $L(-\mathrm{TA})$ and $L(-\mathrm{LA})$. In Fig. 1, the $L(-\mathrm{TA})$ transition begins to emerge at 19°K, and in Fig. 3, where a thicker sample (5.0 mm) was used to enhance the low-level absorption structure, both $L(-\mathrm{TA})$ and $L(-\mathrm{LA})$ are clearly visible. The center of gravity of the pair $L(+\mathrm{TA})$ and $L(-\mathrm{TA})$ or the pair $L(+\mathrm{LA})$ and $L(-\mathrm{LA})$, determines the exciton gap at L, and also gives the TA and LA pho-

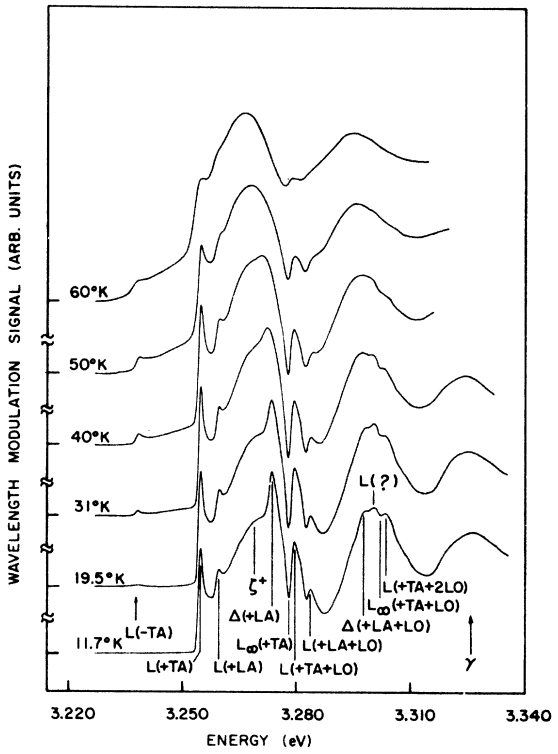

FIG. 1. Wavelength-modulation spectrum of AgCl for temperatures ranging from 11.7 to 60°K. Scale of energy on the abscissa is appropriate only for the 11.7°K data—the spectra for $T > 11.7$°K have been artificially displaced in order that the peaks $L(+\mathrm{TA})$ all line up. See text for details.

non energies. At 6.8°K the exciton gap at L is 3.2468 ± 0.0005 eV. The TA and LA phonon energies throughout the temperature range investigated are 7.9 ± 0.5 and 12.4 ± 0.5 meV, respectively. These results are in excellent agreement with data of previous authors.[3,8] In addition to the single-phonon transitions, higher-order processes can occur involving more than one phonon, provided momentum is still conserved. The structures labeled $L(+\mathrm{TA}+\mathrm{LO})$, $L(+\mathrm{LA}+\mathrm{LO})$, and $L(+\mathrm{TA}+2\mathrm{LO})$ are such transitions, where in addition to a TA or LA phonon at L, either one or two LO phonons with $k \approx 0$ have been emitted. This assignment is supported by the temperature dependence shown in Fig. 2, where it is seen that all of the previously mentioned peaks move rigidly with temperature, and from the fact that the separation of the peaks is predicted very well from the known values of the LO phonon energy.[5,9,10] The LO phonon energy deduced from the WM results is 25.0 ± 0.5 meV, which is to be compared with neutron scattering data at liquid-nitrogen temperature (LNT[5]) (23.8 meV), ir absorption both at helium[9] (24.4 meV), and room temperature[11,12] (24.2 meV), and the results of Raman scattering[10] (24.2 ± 2 meV).

In analogy to the wavelength-modulation results of AgBr,[13] the deep valley, labeled $L_\infty(+\mathrm{TA})$, is speculatively assigned to be the series limit of the exciton since it is expected that the WM signal should go to zero at this point; the binding energy associated with the exciton at L is therefore approximately 23 meV. This should be compared with the binding energy of an electron to a fixed impurity[9] (33 meV). The assignment $L_\infty(+\mathrm{TA}+\mathrm{LO})$ to the series limit of $L(+\mathrm{TA}+\mathrm{LO})$ is further speculation.

From Fig. 2 it is evident that the structures labeled $\Delta(+\mathrm{LA})$ and $\Delta(+\mathrm{LA}+\mathrm{LO})$ shift with respect to $L(+\mathrm{TA})$ as the temperature is varied, suggesting that these transitions are not associated with the valence-band maximum at L. The band calculations of Bassani *et al.*[1] predict subsidiary valence-band maxima along ⟨110⟩ and along ⟨100⟩ which are nearly degenerate with the valence-band max-

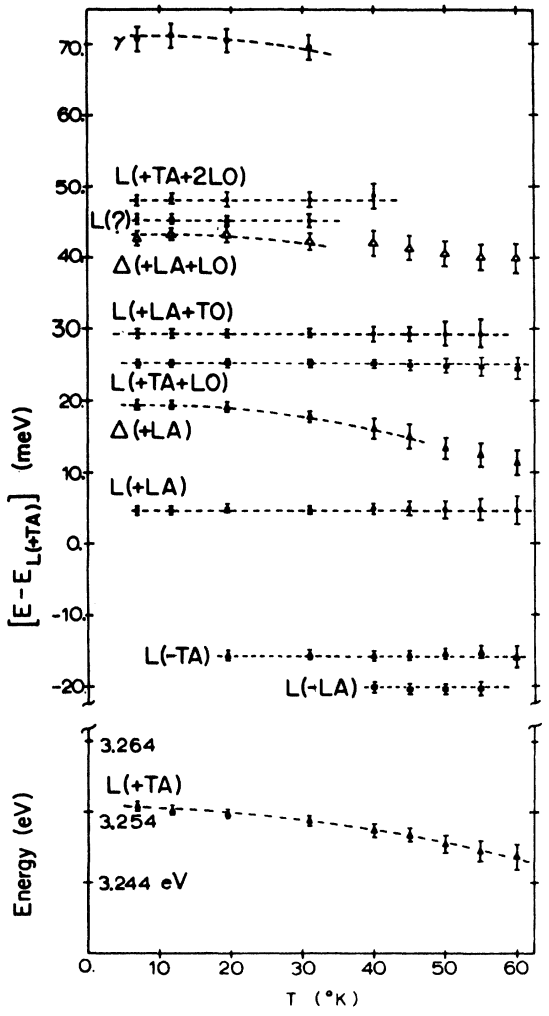

FIG. 2. Temperature dependence of the relative separation between $L(+\mathrm{TA})$ and the remaining structure of Fig. 1. In the lower portion is plotted the absolute energy of the $L(+\mathrm{TA})$ line as a function of temperature.

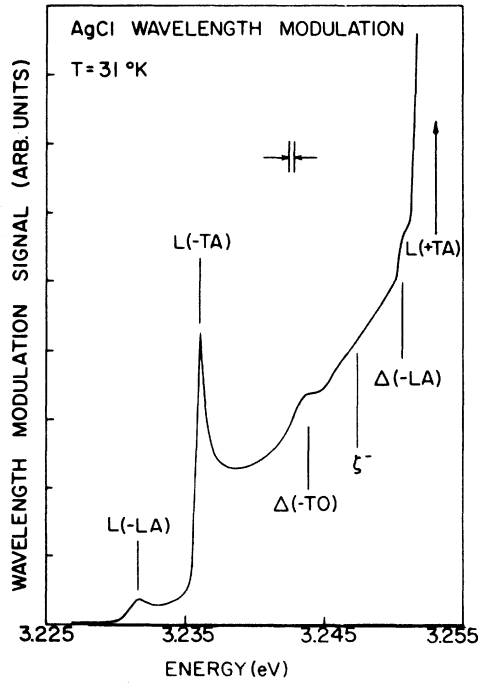

FIG. 3. Wavelength-modulation signal of an ~5-mm thick AgCl sample at $T = 31$ °K showing phonon absorption structure.

imum at L. We assign the structure $\Delta(+\mathrm{LA})$ and $\Delta(+\mathrm{LA}+\mathrm{LO})$ to transitions originating from the subsidiary maximum at Δ, along $\langle 100\rangle$.

Support for this assignment comes from the observation, at 6.8°K, of structure on the high-energy side of $L(+\mathrm{TA}+\mathrm{LO})$ labeled $\Delta(+\mathrm{TO})$ in Fig. 4, and the appearance at higher temperatures of new structure labeled $\Delta(-\mathrm{LA})$ and $\Delta(-\mathrm{TO})$ shown in Fig. 3. As the labeling suggests, we have assigned this structure to the formation of excitons in which the electronic transition originates from the valence band at Δ and either an LA or TO phonon at Δ is absorbed or emitted. Selection rules restrict the momentum conserving phonons that participate in the transition from the valence-band maximum at L_3^- to the conduction-band minimum at Γ_1^+ to LA and TA phonons; in the case of transitions from Δ_1 to Γ_1^+ all phonons of the appropriate wave vector contribute to the transition probability. The phonon absorption peaks $\Delta(-\mathrm{LA})$ and $\Delta(-\mathrm{TO})$ shown in Fig. 3 are resolved only over a small temperature range due to strong broadening for temperatures larger than approximately 35°K. The center of gravity of the pair $\Delta(+\mathrm{LA})$ and $\Delta(-\mathrm{LA})$ is identical to that for $\Delta(+\mathrm{TO})$ and $\Delta(-\mathrm{TO})$, and gives a value of 3.2640 ± 0.0005 eV for the gap associated with exciton formation at Δ for $T=6.8$°K. From this we also deduce the LA and TO phonon energies at Δ to be $10.0+0.5$ and $17.0+0.5$ meV, respectively.

A conclusive identification of these phonons as being those at Δ must come from a measure of both their energy and their wave vector. From the measured phonon dispersion curves,[5] 10.0- and 17.0-meV phonons occur both at approximately $(0.53,0,0)(2\pi/a)$ in the $\langle 100\rangle$ direction and at approximately $(0.35,0.35,0)(2\pi/a)$ in the $\langle 110\rangle$ direction. The band-structure calculations[1,2] show valence-band maxima (in addition to the maximum at L) at approximately $(0.51,0,0)(2\pi/a)$ in the $\langle 100\rangle$ direction, at approximately $(0.67,0.67,0)(2\pi/a)$ in the $\langle 110\rangle$ direction, and at the point W, $(0.5,1,0)\times(2\pi/a)$. In the case of AgCl, momentum conservation requires that for an indirect transition the phonon wave vector must be equal to the wave vector associated with the particular valence-band maximum from which the transition originates. In the absence of unusual behavior of the phonon dispersion, the measured phonon energies do not appear to be consistent with the third alternative above, i.e., a subsidiary valence-band maximum at W. The assignment of the wave vector of the above 10.0-and 17.0-meV phonons (and hence of the symmetry of the subsidiary valence-band maximum) as being associated with Δ is therefore the alternative which is the most compatible with both the phonon dispersion data and the band-structure calculations.

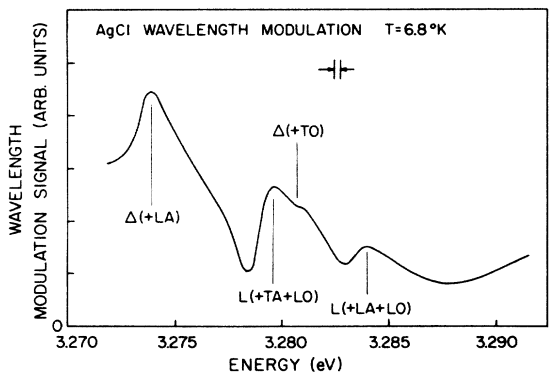

FIG. 4. Wavelength-modulation signal of 0.5-mm AgCl sample at $T=6.8$°K under high resolution. Note that the energy axis has been expanded in comparison with Fig. 1.

Recently, a new band structure has been proposed by Tejeda *et al.*[14] which exhibits a new degeneracy of the conduction-band minima at X and Γ (which is absent in the previous calculations[1,2]), and a near degeneracy of the valence-band maxima at L and Σ. The valence-band maxima at Σ and Δ occur at the same wave vector in the Brillouin zone in their calculation as in the calculation of both Scop[2] and Bassani *et al.*[1] The valence-band maximum at Δ, however, is shown to be approximately 0.5 eV below the maximum at L.

This band structure introduces the possibility of an indirect exciton created by a transition from the valence-band maximum at L to the conduction-band minimum at X. Such a transition requires a momentum conserving phonon with q along $\langle 111\rangle$ whose energy would be the same as that of the phonons contributing to the L exciton transition. The phonon energies we have measured are not compatible with such a possibility.

We have examined the present results in light of the polaron effects seen in the absorption edge of AgBr,[13] where structure occurs at an energy equal to the energy of the absorption threshold plus nearly the electron polaron self-energy. In AgBr, the transition is a higher-order process which involves first a phonon-assisted transition to an intermediate virtual state in which the exciton is at rest and the electron is undressed, followed by either the emission or absorption of an acoustic phonon to a final state in which the exciton has nonzero kinetic energy and the electron is dressed. The threshold for this process, relative to the initial absorption edge, is the electron polaron self-energy plus (minus) the energy of the phonon emitted (absorbed) in going from the intermediate virtual state to the final state.

Perturbation theory[15] gives the electron polaron self-energy E_{se} as

$$E_{se}^{(pert)} = \alpha\hbar\omega(1+0.0159\alpha),$$

where α is the electron phonon coupling constant and $\hbar\omega$ is the LO phonon energy. Larsen's[16] value for the self-energy, calculated using a variational technique, differs from $E_{se}^{(pert)}$ by an amount that is not detectable in the present measurements. For $\alpha = 1.885$ and $\hbar\omega = 23.8$ meV, the self-energy of the polaron is $E_{se}^{(pert)} = 46.2$ meV. We expect, then, to see some kind of a resonance at an energy of $(E_{se}^{(pert)} \pm \delta)$ relative to $L(+\mathrm{TA})$, where δ is the energy of the phonon emitted or absorbed in going to the final dressed state. For an assumed hole mass between 0 and $3m_e^*$, the energy δ, of such an LA phonon, varies between approximately 3.4 and 2.6 meV. At low temperature, we would expect to see structure at an energy $E_{se}^{(pert)} + \delta \cong 49$ meV above $L(+\mathrm{TA})$. The situation is, however, complicated by the fact that in the same region of energy, we expect to find the one LO phonon replica of $L_\infty(+\mathrm{TA})$ and the two LO phonon replicas of $L(+\mathrm{TA})$. It is likely that there may be an interaction between the polaron state and the above-mentioned nearly degenerate states which could lead to a lowering of the energy associated with the expected polaron resonance. It is therefore possible that the structure labeled $L(?)$ in Fig. 1, is in fact associated with the electron polaron self-energy. It should be stressed, however, that the exact nature of this peak is not well established at present. A summary of the relevant energies measured in this work is given in Table I.

TABLE I. Summary of the energies of the exciton gaps at L and Δ, and of the energies of the various momentum-conserving phonons as determined from the wavelength-modulation spectra shown in Fig. 1.

Exciton gap energies	
Exciton gap (L)	3.2468 ± 0.0005 eV; $T = 6.8$ °K
Exciton gap (Δ)	3.2640 ± 0.0005 eV; $T = 6.8$ °K
Phonon energies	
TA(L)	7.9 ± 0.5 meV
LA(L)	12.4 ± 0.5 meV
LO(Γ)	25.0 ± 0.5 meV
LA(Δ)	10.0 ± 0.5 meV
TO(Δ)	17.0 ± 0.5 meV

IV. LINE SHAPE

In analyzing the line shape of the wavelength-modulation spectrum, it is convenient to conceptualize the absorption coefficient $\alpha(\lambda)$ as a sum of partial absorption coefficients $\alpha_i(\lambda)$, each corresponding to a single absorption process

$$\alpha(\lambda) = \sum_i \alpha_i(\lambda).$$

We can then calculate the line shape associated with each type of absorption process separately, and then simply add up our results in order to compare them with experiment.

In Sec. IV A, we determine the line shape corresponding to free indirect exciton formation for a simple parabolic exciton band in which the kinetic energy of the exciton is quadratic in the momentum, and then proceed, in Sec. IV B, to calculate the same line shape for the case in which an interaction between exciton bands is included.

A. Parabolic band

In an indirect gap material such as AgCl, the absorption coefficient due to phonon-assisted free exciton formation[13] is proportional to $(E - E_0)^{1/2}$ where E is the energy of the incident photon and E_0 is the absorption threshold given by $E_0 = E_g \pm \hbar\omega_{ph}$. This dependence reflects the density of states of the center of mass of the free exciton. E_g is the indirect exciton gap energy and $\hbar\omega_{ph}$ is the energy of the momentum conserving phonon. Since the wavelength-modulation signal is proportional to the derivative of the absorption coefficient, we would expect to see a line shape similar to $(E - E_0)^{-1/2}$ associated with indirect exciton formation. Owing to the finite bandwidth of the experimental apparatus and to the finite lifetime of both the exciton and phonon, the singularity at $E = E_0$ is in practice never observed. To account for lifetime broadening we must go back to the energy dependence of the absorption coefficient and introduce a complex energy,

$$(E - E_0)^{1/2} \to (E - E_0 + i\delta)^{1/2}. \tag{1}$$

The real part of this function represents the energy dependence of the absorption coefficient where the final state reached during optical absorption has a lifetime that is inversely proportional to δ.[17] Taking the real part of Eq. (1) gives for the absorption coefficient α

$$\alpha \propto \mathrm{Re}(E - E_0 + i\delta)^{1/2} = [(E - E_0)^2 + \delta^2]^{1/4} \cos\tfrac{1}{2}\theta, \tag{2}$$

where

$$\theta = \begin{cases} \tan^{-1}(\delta/E - E_0), & E \geq E_0, \\ \tfrac{1}{2}\pi + \tan^{-1}[(E_0 - E)/\delta], & E \leq E_0. \end{cases} \tag{3}$$

This line shape is shown as curve (a) in Fig. 5. The derivative of the expression in Eq. (2) is then proportional to the wavelength-modulation signal

$$\frac{d\alpha}{dE} \propto \tfrac{1}{2}[(E-E_0)^2+\delta^2]^{-3/4}[(E-E_0)\cos\tfrac{1}{2}\theta+\delta\sin\tfrac{1}{2}\theta]\,. \tag{4}$$

This line shape is shown as curve (a) in Fig. 6. The position of the peak of this curve depends both on E_0 and on the amount of broadening present. Taking the derivative of Eq. (4) and setting the result equal to zero, gives the dependence of the peak position on these parameters

$$E_{\text{peak}} = E_0 + \delta/\sqrt{3}\,. \tag{5}$$

This result is useful in interpreting the data since the threshold E_0 can be determined from the observed peak provided a reasonable estimate for δ can be made.

B. Nonparabolic band

If the exciton dispersion is nonparabolic, then Eq. (2) is no longer appropriate and the observed line shape for the absorption coefficient will deviate from the simple square-root energy dependence of Eq. (1). Nonparabolic effects have been investigated recently in germanium[18,19] for the case of degenerate exciton bands, and also in the case of nitrogen doped semiconductor alloys (e.g., $GaAs_{1-x}P_x$ and $In_{1-x}Ga_xP$), where the resonant impurity state interacts with the exciton band.[20] The same general procedure used in the study of the interaction of electrons with a localized impurity[21] will be followed here.

In this section, we consider nonparabolic effects induced by the interaction of two nearly degenerate exciton bands separated in k space by a wave vector q. We shall then calculate the energy dependence of the absorption coefficient α in the presence of the electron interaction that mixes these exciton bands. The matrix elements which describe this interaction can be expanded in a series of both q and $1/q$. The former is predominant when q is large. The first term of this expansion is the well-known deformation potential coupling. For AgCl, the WM measurements show that there is an exciton band at Δ, $(0.53,0,0)(2\pi/a)$, and at L, $(0.5,0.5,0.5)(2\pi/a)$, separated by approximately 17 meV and by a wave vector of approximately $(0,0.5,0.5)(2\pi/a)$. The new exciton wave function at L, $|\psi_L(k)\rangle$, in the presence of this mixing is given in terms of the unperturbed wave functions at L and Δ by

$$|\psi_L(k)\rangle = a\,|0,\psi_L^0(k)\rangle + \sum_{k'} b_{k'}\,|q,\psi_\Delta^0(k')\rangle\,. \tag{6}$$

Here k and k' refer, respectively, to the exciton bands at L and Δ, where in each case the momentum is measured relative to the respective exciton band minimum; and q is the wave vector of the pho-

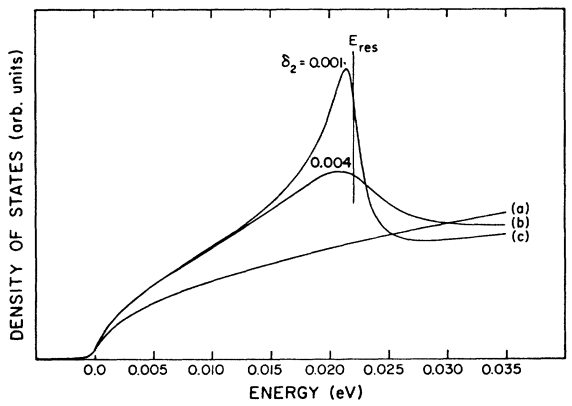

FIG. 5. Energy dependence of the density of states (dos) of the L exciton band. Curve (a) represents the dos given by Eq. (2) associated with a simple parabolic exciton band. Curves (b) and (c) represent the calculated dos of the perturbed L exciton band given by Eq. (30) for two values of the broadening parameter δ_2. The zero of energy is taken to be at the L exciton band minimum.

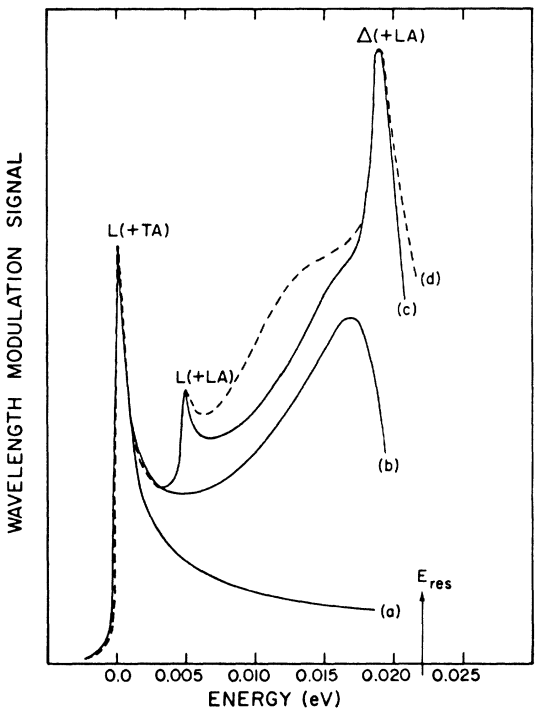

FIG. 6. Calculated wavelength-modulation line shapes (solid lines) and the experimentally observed wavelength-modulation line shape at 6.8 °K (dashed line). Curve (a) represents the derivative of Eq. (2). Curve (b) represents the derivative of Eq. (30) and curve (c) is the sum of the calculated line shapes associated with L (+TA), L(+LA), and Δ(+LA) (parameter values used: $\delta_1 = 0.18$ meV, $\delta_2 = 4.0$ meV). See text for details.

non required to mix the exciton bands. The unperturbed wave function $|q, \psi_i^0(k)\rangle$ refers to a state of the crystal in which there is a phonon of wave vector q and an exciton of wave vector k, where k is measured from the ith exciton band minimum. The Hamiltonian which describes this system is

$$H = H_0 + H' . \tag{7}$$

where the following relations for H_0 hold.

$$H_0 |0, \psi_L^0(k)\rangle = [E_L^0 + (\hbar k)^2/2m_L] |0, \psi_L^0(k)\rangle , \tag{8a}$$

$$H_0 |q, \psi_\Delta^0(k')\rangle = [E_\Delta^0 + (\hbar k')^2/2m_\Delta \pm \hbar\omega_q] |q, \psi_\Delta^0(k')\rangle . \tag{8b}$$

We will consider here only the plus sign for the phonon energy in Eq. (8b), since only phonon emission is expected to be important at low temperatures. The dispersion of the L exciton band is determined by solving the Schrödinger equation

$$H |\psi_L(k)\rangle = E_L(k) |\psi_L(k)\rangle . \tag{9}$$

Substituting Eqs. (6)–(8) into Eq. (9) we obtain

$$a\left(E_L^0 + \frac{(\hbar k)^2}{2m_L}\right) + \sum_{k'} b_{k'}\beta^* = aE_L \tag{10}$$

and

$$\beta a + [E_\Delta^0 + (\hbar k')^2/2m_\Delta + \hbar\omega_q] b_{k'} = b_{k'} E_L , \tag{11}$$

where

$$\beta = \langle q, \psi_\Delta^0(k') | H | 0, \psi_L^0(k)\rangle . \tag{12}$$

Calculating $b_{k'}$ from Eq. (11) and substituting into Eq. (10) gives

$$E_L - \left(E_L^0 + \frac{(\hbar k)^2}{2m_L}\right) = \sum_{k'} \frac{\beta^2}{E_L - E_\Delta^0 - (\hbar k')^2/2m_\Delta - \hbar\omega_q} . \tag{13}$$

Converting the sum over k' to an integral gives

$$E_L - \left(E_L^0 + \frac{(\hbar k)^2}{2m_L}\right) = \frac{-Vm_\Delta\beta^2}{\hbar^3\pi^2} \int \frac{(\hbar k')^2 d(\hbar k')}{(E_\Delta^0 + \hbar\omega_q - E_L)2m_\Delta + (\hbar k')^2} , \tag{14}$$

where V is the volume of the unit cell. Integrating the right-hand side we obtain

$$E_L = E_L' + (\hbar k)^2/2m_L + \chi , \tag{15}$$

where

$$E_L' = E_L^0 - Vm_\Delta\beta^2 k'/\hbar^2\pi^2 \tag{16}$$

and

$$\chi = \begin{cases} \dfrac{Vm_\Delta\beta^2}{\hbar^3\pi^2}[2m_\Delta(\hbar\omega_q + E_\Delta^0 - E_L)]^{1/2} \tan^{-1}\dfrac{\hbar k'}{[2m_\Delta(\hbar\omega_q + E_\Delta^0 - E_L)]^{1/2}} & \text{for } E_L < \hbar\omega_q + E_\Delta^0 , \quad (17a) \\ \dfrac{-Vm_\Delta\beta^2}{2\hbar^3\pi^2}[2m_\Delta(E_L - \hbar\omega_q - E_\Delta^0)]^{1/2} \ln\dfrac{\hbar k' - [2m_\Delta(E_L - \hbar\omega_q - E_\Delta^0)]^{1/2}}{\hbar k' + [2m_\Delta(E_L - \hbar\omega_q - E_\Delta^0)]^{1/2}} & \text{for } E_L > \hbar\omega_q + E_\Delta^0 . \quad (17b) \end{cases}$$

From the results given by Eqs. (15) and (16), we see that the energy E_L, of the perturbed L exciton band, is equal to the energy of the unperturbed band shifted rigidly downward by a constant amount equal to $Vm_\Delta\beta^2 k'/\hbar^2\pi^2$, plus a small energy-dependent term χ. It is the term χ which introduces the nonparabolicity of the exciton band, and it is the effect of this term on the absorption coefficient which we wish to determine.

A first-order estimate for the rigid shift of the exciton band can be made using the deformation potential approximation for H', i.e., $H' = \mathcal{E}_d \nabla\cdot\mathfrak{u}$. Here $\mathcal{E}_d$ is the deformation potential constant and $\nabla\cdot\mathfrak{u}$ is the dilation of the lattice. Measurements of the changes of the absorption threshold with hydrostatic pressure give $\mathcal{E}_d \cong 0.5$ eV.[22] Using this value we find $\beta \cong 10$ meV and $E_L' - E_L^0 \sim 0.1$ meV. This is reasonable even though H' and $\mathcal{E}_d$ only apply to $q \approx 0$ phonons.

The dispersion of the exciton band given by Eq. (15) is reflected in the absorption coefficient through the energy dependence of the density of states. We now calculate the density of states $D(E)$ using the relation

$$k^2 dk = D(E) dE . \tag{18}$$

Differentiating Eq. (15) gives

$$\frac{dE_L}{d(\hbar k)} = \frac{\hbar k}{m_L} + \frac{d\chi}{dE_L}\frac{dE_L}{d\hbar k} , \tag{19}$$

from which we obtain

$$dk = \frac{m_L}{\hbar^2 k}\left(1 - \frac{d\chi}{dE_L}\right) dE_L . \tag{20}$$

For large k' and $E_L < E_\Delta^0 + \hbar\omega_q$, χ as given by Eq. (17a) is

$$\chi = \tfrac{1}{2} A\pi[2m_\Delta(E_\Delta^0 + \hbar\omega_q - E_L)]^{1/2} , \tag{21}$$

where

$$A = Vm_{\Delta}\beta^2/\hbar^3\pi^2 . \tag{22}$$

Substituting Eq. (21) into Eq. (20) and then multiplying through by k^2 gives

$$k^2\,dk = \frac{m_L k}{\hbar^2}\left(1+\frac{A\pi m_{\Delta}}{2[2m_{\Delta}(\hbar\omega_q + E_{\Delta}^0 - E_L)]^{1/2}}\right)dE_L . \tag{23}$$

For χ small, Eq. (15) gives

$$k = (1/\hbar)[(E_L - E_L')2m_L]^{1/2} . \tag{24}$$

Using Eq. (24) in Eq. (23) and letting $E_L = E_L' + \mathcal{E}$, we obtain the following form for the density of states for $E_L < (E_{\Delta}^0 + \hbar\omega_q - E_L^0)$:

$$D(\mathcal{E}) = D_0(\mathcal{E}) + D_1(\mathcal{E}) = \mathcal{E}^{1/2}\left(a_0 + \frac{a_1}{[\hbar\omega_q + E_{\Delta}^0 - E_L^0 - \mathcal{E}]^{1/2}}\right), \tag{25}$$

where $D_0(\mathcal{E}) = a_0\mathcal{E}^{1/2}$ and a_0 and a_1 are constants.

Similarly, substituting the form of χ given in Eq. (17b) {where $\hbar k' \gg [2m_{\Delta}(E_L - \hbar\omega_q - E_{\Delta}^0)]^{1/2}$} into Eq. (20), we obtain the density of states for energies larger than $E_{\Delta}^0 + \hbar\omega_q - E_L^0$:

$$D(\mathcal{E}) = D_0(\mathcal{E}) + D_2(\mathcal{E}) = \mathcal{E}^{1/2}\left(a_0 - \frac{8a_2}{\pi}\frac{(2m_{\Delta})^{1/2}}{\hbar k'}\right), \quad \mathcal{E} > E_{\Delta}^0 + \hbar\omega_q - E_L^0 . \tag{26}$$

The expressions given in Eqs. (25) and (26) each contain a term, $D_0(\mathcal{E})$, that is equal to the "usual" density of states which is observed in the absence of any exciton band interaction and, second, a term, $D_1(\mathcal{E})$ or $D_2(\mathcal{E})$, which can be described as the added density of states due to the interaction of the two bands. It is clear from Eq. (25), that on account of the resonant denominator, the added density of states becomes increasingly important as $\mathcal{E}$ approaches $E_{\rm res} = E_{\Delta}^0 + \hbar\omega_q - E_L^0$. As $\mathcal{E}$ approaches $E_{\rm res}$ from below, the added density of states approaches $+\infty$, whereas as $\mathcal{E}$ approaches $E_{\rm res}$ from above, the added density of states approaches

$$-8a_2E_{\rm res}^{1/2}[(2m_{\Delta})^{1/2}/\pi\hbar k'] .$$

The parameter k' which appears in Eq. (26), describes the extent of the Δ exciton band that is mixed with the L exciton band. In the limit as k' goes to zero, i.e., where only the lowest state in the Δ exciton band is mixed, the added density of states goes to $-\infty$ as $\mathcal{E}$ approaches $E_{\rm res}$ from above. This would be the result for a discrete scattering state.[21]

We can again take into account lifetime-broadening effects in the same way as was done for the case of a parabolic exciton band, by taking the real part of the functions given by Eqs. (25) and (26) when the energy is complex. This procedure is tedious but straightforward and gives the following result. Equation (25) becomes

$$D_0(\mathcal{E}) + D_1(\mathcal{E}) = (\mathcal{E}^2 + \delta_1^2)^{1/4}\{a_0 + a_1(\cos\tfrac{1}{2}\phi)/[(E_{\rm res} - \mathcal{E})^2 + \delta_2^2]^{1/4}\}\cos\tfrac{1}{2}\theta , \tag{27}$$

where

$$\theta = \begin{cases} \tan^{-1}(\delta_1/\mathcal{E}), & \mathcal{E} > 0, \\ \tfrac{1}{2}\pi + \tan^{-1}(-\mathcal{E}/\delta_1), & \mathcal{E} < 0; \end{cases}$$
$$\phi = \begin{cases} \tan^{-1}[\delta_2/(E_{\rm res} - \mathcal{E})], & \mathcal{E} < E_{\rm res}, \\ \tfrac{1}{2}\pi + \tan^{-1}[(\mathcal{E} - E_{\rm res})/\delta_2], & \mathcal{E} > E_{\rm res} . \end{cases} \tag{28}$$

The added density of states above $E_{\rm res}$ given by $D_2(\mathcal{E})$ becomes

$$D_2(\mathcal{E}) = (-8/\pi)[(2m_{\Delta})^{1/2}/\hbar k']a_2(\mathcal{E}^2 + \delta_1^2)^{1/4}\cos\tfrac{1}{2}\theta , \tag{29}$$

where θ is given by Eq. (28). The complete density of states which gives the line shape associated with the absorption coefficient is then

$$D(\mathcal{E}) = D_0(\mathcal{E}) + D_1(\mathcal{E}) + D_2(\mathcal{E}) = (\mathcal{E}^2 + \delta_1^2)^{1/4}\left(a_0 + \frac{a_1\cos\tfrac{1}{2}\phi}{[(E_{\rm res} - \mathcal{E})^2 + \delta_2^2]^{1/4}} - \frac{8a_2}{\pi}\frac{(2m_{\Delta})^{1/2}}{\hbar k'}\right)\cos\tfrac{1}{2}\theta . \tag{30}$$

Curve (a) in Fig. 5 shows the broadened square-root line shape, $D_0(\mathcal{E})$, given by Eq. (2), that is expected in the absence of exciton band mixing. Curves (b) and (c) in Fig. 5 show the line shape given by Eq. (30) for two values of the broadening parameter δ_2. In general δ_2 is energy dependent since as resonance is approached, the probability of a real decay into the Δ exciton band becomes large. For simplicity we have taken δ_2 to be constant. The zero in energy in Fig. 5 has been taken to be the absorption threshold which, in this case, is equal to the exciton gap at L. The value of $E_{\rm res}$ shown in this figure, has been determined from the WM measurements which give approximately 17 meV for the energy difference between the Δ and L exciton bands, and from the phonon dispersion curves (Fig. 1 of Ref. 4) which give for the energy of the $(0, 0.5, 0.5)(2\pi/a)$ coupling phonon, a value of

approximately 5 meV. Thus $E_{res} \cong (17+5)\,\text{meV} = 22$ meV.

The predicted WM line shape is given by the derivative of Eq. (30) and is shown in curve (b) of Fig. 6. A comparison of curves (a) and (b) in this figure clearly shows the effect of the nonparabolicity of the exciton band on the wavelength-modulation spectrum. In order to compare our calculated line shape with the experimentally observed line shape, we have included the contributions corresponding to both $L(+\text{TA})$ and $L(+\text{LA})$. Curve (c) in Fig. 6 is the sum of curve (b) and an identical curve which has been displaced towards higher energy in order to line up with the experimentally observed $L(+\text{LA})$ line and which has been scaled in magnitude by approximately $\frac{1}{4}$, the measured ratio of the density of states of the LA and TA phonons.[5] We have also added a component similar to curve (a) for the contribution due to $\Delta(+\text{LA})$. Curve (d) in Fig. 6 is the experimentally observed line shape at 6.8°K.

We feel that the good agreement between curves (c) and (d) provides strong evidence for the existence of the exciton band interaction mechanism which we have described. The agreement is poor, however, in the region for $\mathcal{E}$ close to E_{res} where a strong negative lobe is predicted in the derivative signal. This eventual disagreement close to resonance, which has been investigated for a similar case in the calculation of the polaron dispersion,[23] may be due in part to the neglect of multiphonon processes. We speculatively assign the structure γ (in Fig. 1) as well as the broad structure that appears to underly $\Delta(+\text{LA}+\text{LO})$, $L(?)$, and $L(+\text{TA}+2\text{LO})$ to replicas of this resonance displaced by one or two LO phonons.

We have considered the possibility that the broad shoulder $\zeta+$ in the WM spectrum which is assigned to the nonparabolicity of the exciton band due to an interband electron phonon interaction may instead be due to either intraband polaron effects, to interaction with some unknown impurity, or to transitions to some type of a localized exciton state. From the temperature dependence of the spectrum, it is seen that the shoulder $\zeta+$ which appears between $L(+\text{TA})$ and $\Delta(+\text{LA})$, moves with the exciton band at Δ. This rules out a polaron effect since in this case one would not expect this structure to move with respect to $L(+\text{TA})$ (the LO phonon energy is essentially constant over the temperature range investigated and the LO phonon population is negligible for $T \lesssim 80$°K). A second important feature of the WM spectrum is that a shoulder similar to $\zeta+$ also appears in phonon absorption ($\zeta-$) between $L(-\text{TA})$ and $\Delta(-\text{LA})$. This is contradictory with an assignment to a localized state, since such a transition does not require a momentum conserving phonon.

We have examined a variety of different samples in order to identify possible extrinsic sources of this shoulder. We have seen the same line shape in both zone-refined and non-zone-refined material[24] and in samples left in either a fluorine, bromine, or iodine atmosphere at 80°C for approximately one week.[25] No difference was found in samples annealed in either a helium or a chlorine atmosphere. These results indicate that neither metal impurities nor the above-mentioned isoelectronic impurities are likely to be associated with $\zeta+$. Finally, while the simultaneous application of red light changes the population of filled traps associated with the Δ minimum, it does not modulate the absorption spectrum. The results of the photoconductivity spectra will be treated in a successive publication.

V. CONCLUSION

We have presented the experimental results of a study of the temperature dependence of the indirect absorption edge in AgCl. The results show that in addition to the principle maximum at L, there is also a nearly degenerate subsidiary valence-band maximum at Δ. The energies of the L and Δ exciton gaps at 6.8°K as well as the energies of the various momentum conserving phonons are summarized in Table I. It is to be stressed that although after creation, the exciton is self-trapped[26,27] (on account of the self-trapping of the hole) the absorption data are characteristic of free exciton formation.

In order to explain the observed line shape, we have postulated a phonon induced interaction between exciton bands. We have shown that the results of a calculation based on such a model as applied to the Δ and L exciton bands, is in good agreement with the observed structure, and with the energies of the known phonons in the crystal. This interaction predicts the observed broad shoulder ζ. It predicts that the shoulder ζ should occur both in phonon absorption and phonon emission, and finally that this shoulder should move with the exciton band at Δ as the temperature is varied.

Finally, it is observed in Fig. 1 that the relative amplitude of the peak $\Delta(+\text{LA})$ decreases with respect to both the peak $L(+\text{TA})$ and the shoulder $\zeta+$ as the temperature increases. This is again consistent with the band mixing model, and can be accounted for in terms of the decrease of the energy difference between the L and Δ exciton bands with increasing temperature. As $E_{\Delta}^{0} - E_{L}^{0}$ decreases, there is an increased mixing between the two exciton bands which implies a decreased

density of states associated with the Δ exciton band that is reflected in a decrease of the amplitude of the Δ(+ LA) peak. While the change in amplitude of the Δ(+ LA) line is consistent with the band mixing model, it should be pointed out that this explanation is not unique. The amplitude decrease at high temperature could also be accounted for in terms of a decreased lifetime of the Δ exciton owing to a higher probability of scattering into the L exciton band.

We feel that the phonon induced exciton band mixing should be observed in other materials with nearly degenerate exciton bands. Recent experimental and theoretical results in AgF,[28,29] for example, indicate that perhaps exciton band interaction could be important in this material.

ACKNOWLEDGMENT

The authors would like to thank Professor S. Rodriguez for his critical reading of the manuscript.

*Work supported in part by NSF Grant No. GH-41524 and MRL Program Grant No. DMR72-02018A03.

[1]F. Bassani, R. S. Knox, and W. B. Fowler, Phys. Rev. 137, A1217 (1965).
[2]P. M. Scop, Phys. Rev. 139, A934 (1965).
[3]B. L. Joesten and F. C. Brown, Phys. Rev. 148, 919 (1966).
[4]M. Matsushita, S. Kurita, K. Kobayashi, and T. Masumi, J. Phys. Soc. Jpn. 33, 1177 (1972); Technical Report of ISSP, Ser. A, No. 595 (1973) (unpublished).
[5]P. R. Vijayaraghavan, R. M. Nicklow, H. G. Smith, and M. K. Wilkinson, Phys. Rev. B 1, 4819 (1970).
[6]A. Perregaux and G. Ascarelli, Appl. Opt. 7, 2031 (1968).
[7]C. P. Poole, *Electron Spin Resonance* (Wiley, New York, 1967), Chap. 10.
[8]K. L. Shaklee and J. E. Rowe, in *Proceedings of the Third International Conference on Photoconductivity, Stanford*, edited by E. M. Pell (Pergamon, Oxford, 1969), p. 157.
[9]R. C. Brandt, thesis (University of Illinois, 1967) (unpublished); and R. C. Brandt and F. C. Brown, Phys. Rev. 181, 1241 (1969).
[10]W. von der Osten, Phys. Rev. B 9, 789 (1974).
[11]G. L. Botger and A. L. Geddes, J. Chem. Phys. 46, 3000 (1967).
[12]R. P. Lowndes, Phys. Rev. B 6, 1490 (1972).
[13]G. Ascarelli and J. E. Baxter, Solid. State Commun. 10, 315 (1972).
[14]J. Tejeda, N. J. Shevchik, W. Braun, A. Goldmann, and M. Cardona, Phys. Rev. B 12, 1557 (1975).
[15]D. Pines, in *Polarons and Excitons*, edited by C. G. Kuper and G. D. Whitfield (Oliver and Boyd, London, 1963), p. 43.
[16]D. M. Larsen, Phys. Rev. 172, 967 (1968).
[17]This procedure is equivalent to taking the convolution of $(E-E_0)^{1/2}$ with a Lorentzian which has a half-width at half-maximum equal to δ.
[18]A. Frova, G. A. Thomas, R. E. Miller, and E. O. Kane, Phys. Rev. Lett. 34, 1572 (1975).
[19]E. O. Kane, Phys. Rev. B 11, 3850 (1975).
[20]M. Altarelli, Phys. Rev. B 11, 5031 (1975).
[21]S. Rodriguez, in *Polarons in Ionic Crystals*, edited by J. T. Devreese (North-Holland, Amsterdam, 1972).
[22]R. B. Aust, Phys. Rev. 170, 784 (1968).
[23]G. Whitfield and R. Puff, Phys. Rev. 139, A338 (1965).
[24]The concentrations of metal impurities are significantly reduced in the zone-refined material as opposed to the non-zone-refined material. F. Moser, D. C. Burnham, and H. H. Tippens, J. Appl. Phys. 32, 48 (1961).
[25]Significant doping has been observed in the silver halides under similar conditions—see, for example, R. C. Hansen, thesis (University of Illinois, 1960) (unpublished); J. E. Baxter, thesis (Purdue University, 1972) (unpublished).
[26]C. L. Marquardt, R. T. Williams, and M. N. Kabler, Solid State Commun. 9, 2285 (1971).
[27]H. Kanzaki and S. Sakuragi, Solid State Commun. 9, 1667 (1971).
[28]A. P. Marchetti and G. L. Bottger, Phys. Rev. B 3, 2604 (1971).
[29]R. C. Birtcher, P. W. Deutsch, J. F. Wendelken, and A. B. Kunz, J. Phys. C 5, 562 (1972).